Supplemental Material to:

Debra Akin, S Keisin Wang, Pouran Habibzadegah-Tari, Brian Law, David Ostrov, Min Li, Xiao-Ming Yin, Jae-Sung Kim, Nicole Horenstein, and William A Dunn, Jr

A novel ATG4B antagonist inhibits autophagy and has a negative impact on osteosarcoma tumors

Autophagy 2014; 10(11)
http://dx.doi.org/10.4161/auto.32229

www.landesbioscience.com/journals/autophagy/article/32229

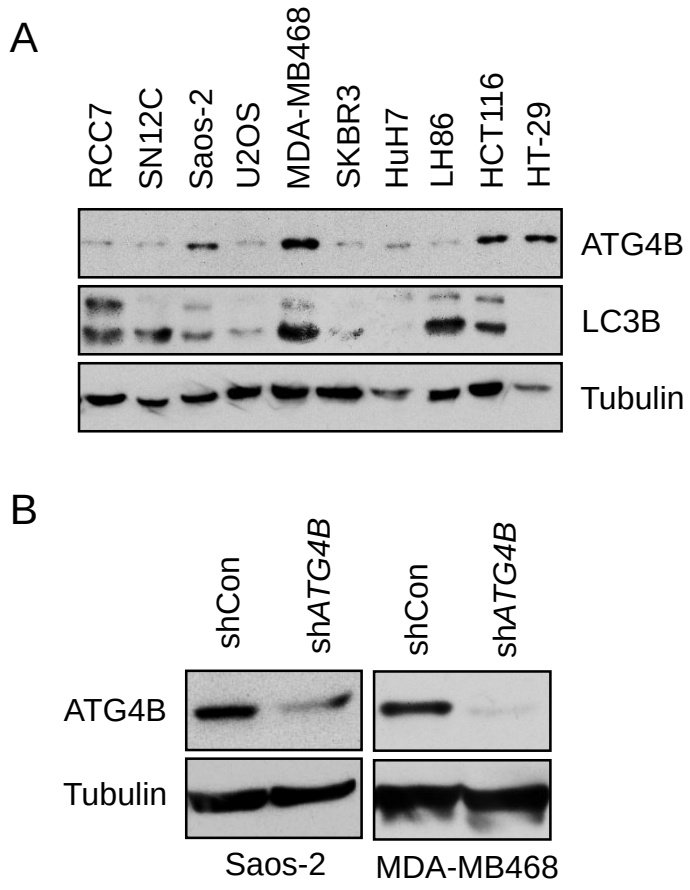

Figure S1. Protein profiles of ATG4B and LC3 in cancer cell lines. (**A**) Human kidney (RCC7 and SN12C), bone (Saos-2 and U2OS), breast (MDA-MB468 and SKBR3), liver (HuH7 and LH86) and colorectal (HCT116 and HT-29) cancer cell lines were cultured under nutrient-rich conditions. The cell lines were solubilized, proteins separated by SDS-PAGE and transferred to PVDF membranes. Afterwards, the membranes were probed with antibodies to ATG4B, LC3B, and β-tubulin. ATG4B was present in almost all the cancers. ATG4B appeared to be truncated in LH86 and HT-29 cells. Under basal conditions, LC3 migrated as 2 bands (LC3-I and LC3-II) in virtually all the cell lines tested. (**B**) shCon and sh*ATG4B* Saos-2 and MDA-MB468 cell lines were solubilized, proteins separated by SDS-PAGE and transferred to PVDF membranes, which were probed with antibodies to ATG4B and β-tubulin.

A

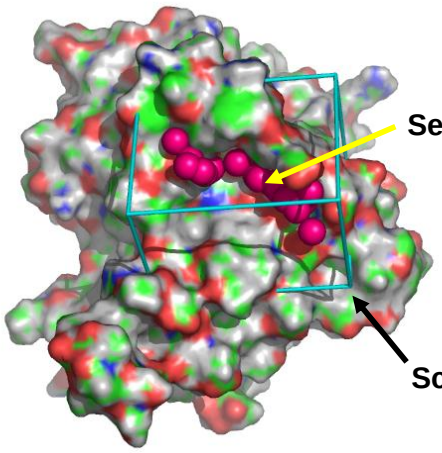

C

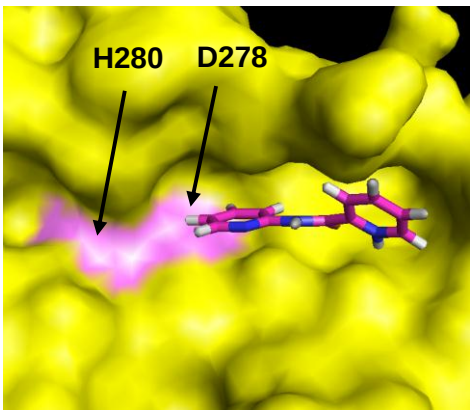

NSC185058

B

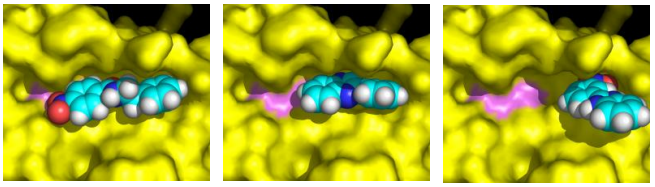

NSC24666 NSC52086 NSC128761

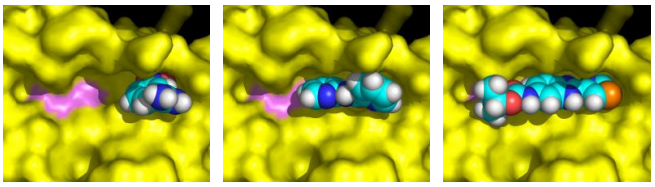

NSC310196 NSC185058 NSC377071

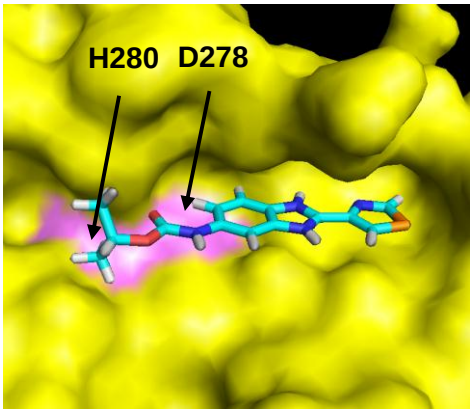

NSC377071

D

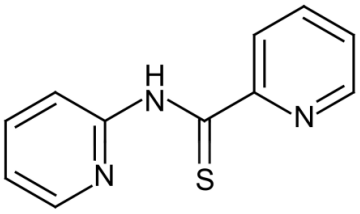

NSC 185058
CAS 39122-38-8
N-pyridin-2-ylpyridine-2-carbothioamide

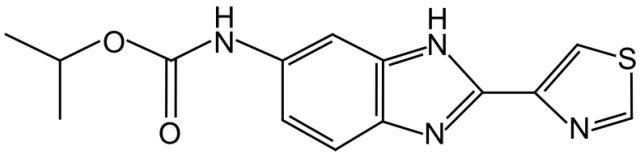

NSC 377071
CAS 26097-80-3
Novazole
Cambendazole
Propan-2-yl N-[2-(1,3-thiazol-4-yl)-3H-benzimidazol-5-yl]carbamate

Figure S2. *In silico* docking of possible ATG4B-targeted compounds into the active site of ATG4B. Upon surveying the crystal structure of ATG4B obtained from the Protein Data Bank, we found that two active site amino acids, D278 and H280, were together within a surface pocket that was accessible for compound docking. (**A**) To run the docking program, the selected site was marked with a scoring grid and spheres as shown. The elements are color coded: red for oxygen, blue for nitrogen, orange for sulfur, and green for carbon. (**B**) The docking of 6 representative compounds is shown. (**C**) The computer-generated positioning of NSC185058 and NSC377071 within the active site pocket of ATG4B is shown. (**D**) The chemical structures of NSC185058 and NSC377071 are shown.

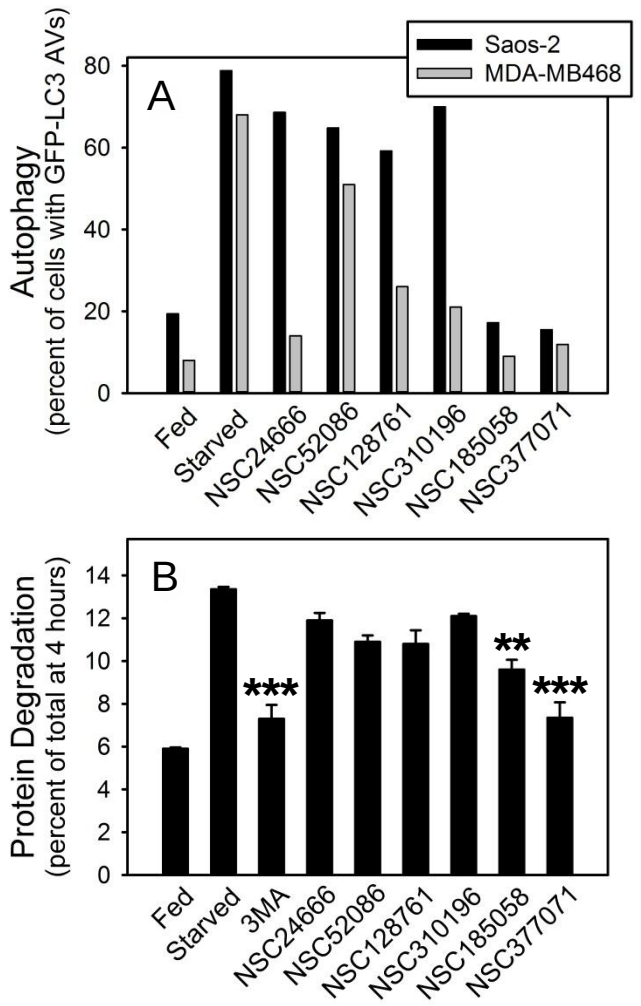

Figure S3. Effects of ATG4B-targeted compounds on starvation-induced autophagy in Saos-2 and MDA-MB468 cell lines. (**A**) Saos-2 and MDA-MB468 cells stably expressing GFP-LC3B were incubated under fed and starved conditions or under starvation conditions in the presence of 100 μM ATG4B-targeted compounds selected by *in silico* docking. The efficacy of these compounds to inhibit starvation-induced autophagy was done by comparing the percentage of autophagy active cells determined by GFP-LC3B labeling within a population of 98 to 227 cells randomly selected from two or more independent experiments. Of the 12 compounds tested (see **Table S1**), NSC185058 and NSC377071 stood out as effective inhibitors of starvation-induced autophagy in both cell types. (**B**) Saos-2 cells were radiolabeled by incubating with ^{14}C-valine and then switched to medium containing amino acids and serum (Fed) or medium depleted of

amino acids and serum (Starved) or starvation medium in the presence of 3-methyladenine (3MA) or ATG4B-targeted compounds, and protein degradation measured as previously described.[1, 2] The values represent the mean ± SEM of 3 or more trials. Statistical comparisons were made to starvation conditions (** $P < 0.01$; *** $P < 0.001$).

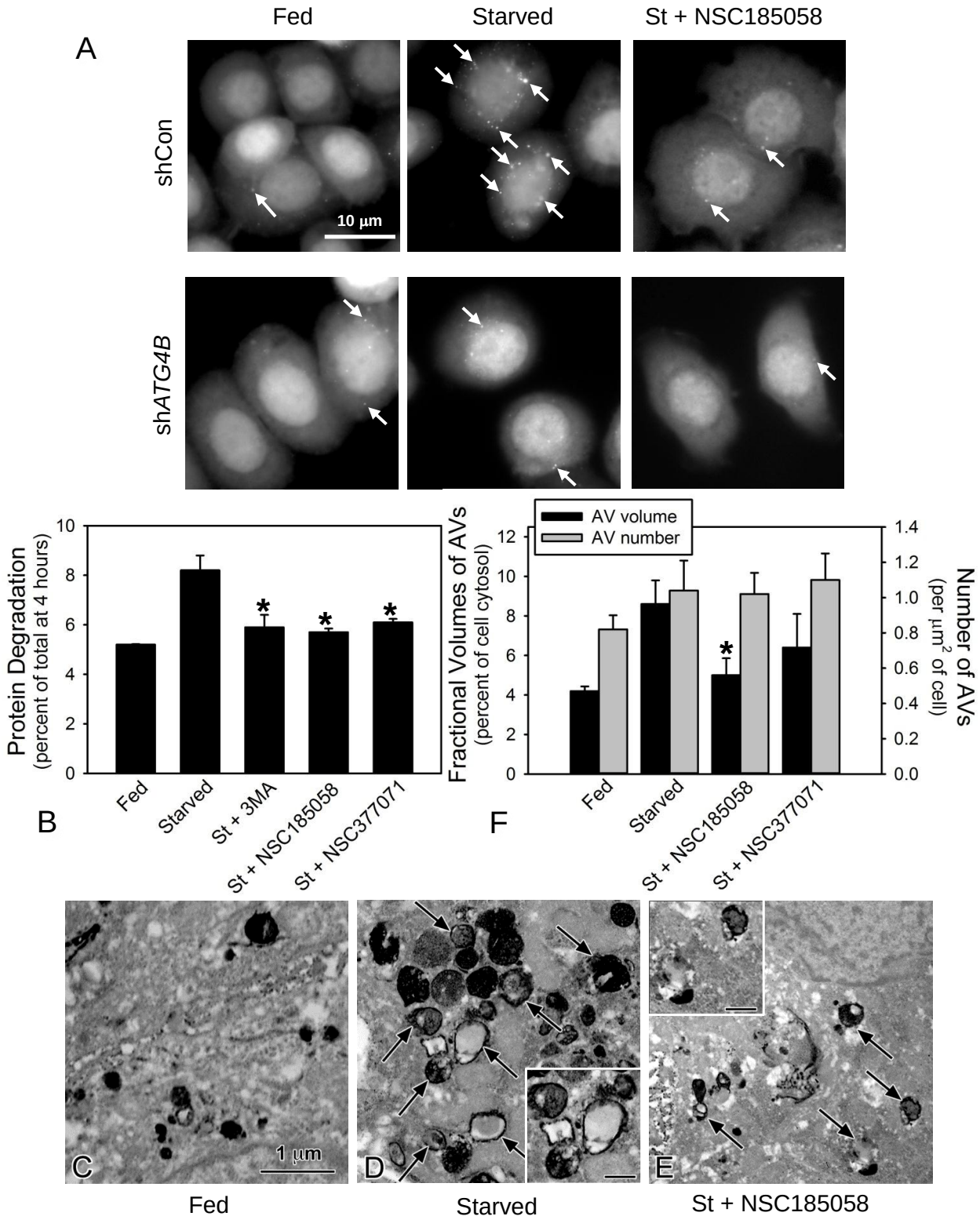
A
Fed
Starved
St + NSC185058
shCon
shATG4B
10 μm
B
Protein Degradation
(percent of total at 4 hours)
Fed
Starved
St + 3MA
St + NSC185058
St + NSC377071
F
AV volume
AV number
Fractional Volumes of AVs
(percent of cell cytosol)
Number of AVs
(per μm2 of cell)
C
D
E
1 μm
Fed
Starved
St + NSC185058

Figure S4. ATG4B-targeted compounds inhibit starvation-induced protein degradation and autophagy in MDA-MB468 cells. (**A**) Stable lines of shCon-MDA-MB468 and sh*ATG4B*-MDA-MB468 expressing GFP-LC3B were incubated in medium enriched for amino acids and serum (Fed) or depleted of amino acids and serum (Starved) or depleted of amino acids and serum in the presence of NSC185058 (St + NSC185058) for 4 h and GFP-LC3B visualized by fluorescence microscopy. GFP-LC3B labeled AVs were present in starved cells that contained ATG4B, but absent from cells lacking ATG4B or treated with NSC185058. Bar (**A**) = 10 μm. (**B**) MDA-MB468 cells were radiolabeled by incubating with ^{14}C-valine for 16 h. Afterwards, the cells were switched to medium containing amino acids and serum (Fed) or medium depleted of amino acids and serum (Starved) in the absence and presence of 3-methyladenine (3MA) or ATG4B-targeted compounds, and levels of protein degraded measured over 4 h relative to total cellular protein.[1, 2] The values represent the mean ± SEM of 3 or more trials. Statistical comparisons were made to starvation conditions (* $P < 0.05$; ** $P < 0.01$; *** $P < 0.001$). (**C to E**) MDA-MB468 cells were incubated under fed (**B**) or starved conditions (**C**) or starved conditions with NSC185058 (**D**). At 4 h, the cells were fixed and processed for CMPase cytochemistry and AVs (arrows) visualized by electron microscopy. The insets contain higher magnifications of representative AVs. Bar (**C to E**) = 1 μm. (**F**) The fractional volumes (black bars) of autophagosomes and autolysosomes were quantified by morphometric techniques and compared to the number of AVs (grey bars) present as previously described.[3, 4] NSC185058 treatment had little effect on the number of AVs, but resulted in a significant reduction in the fractional volumes of AVs compared to starved cells (* $P < 0.05$).

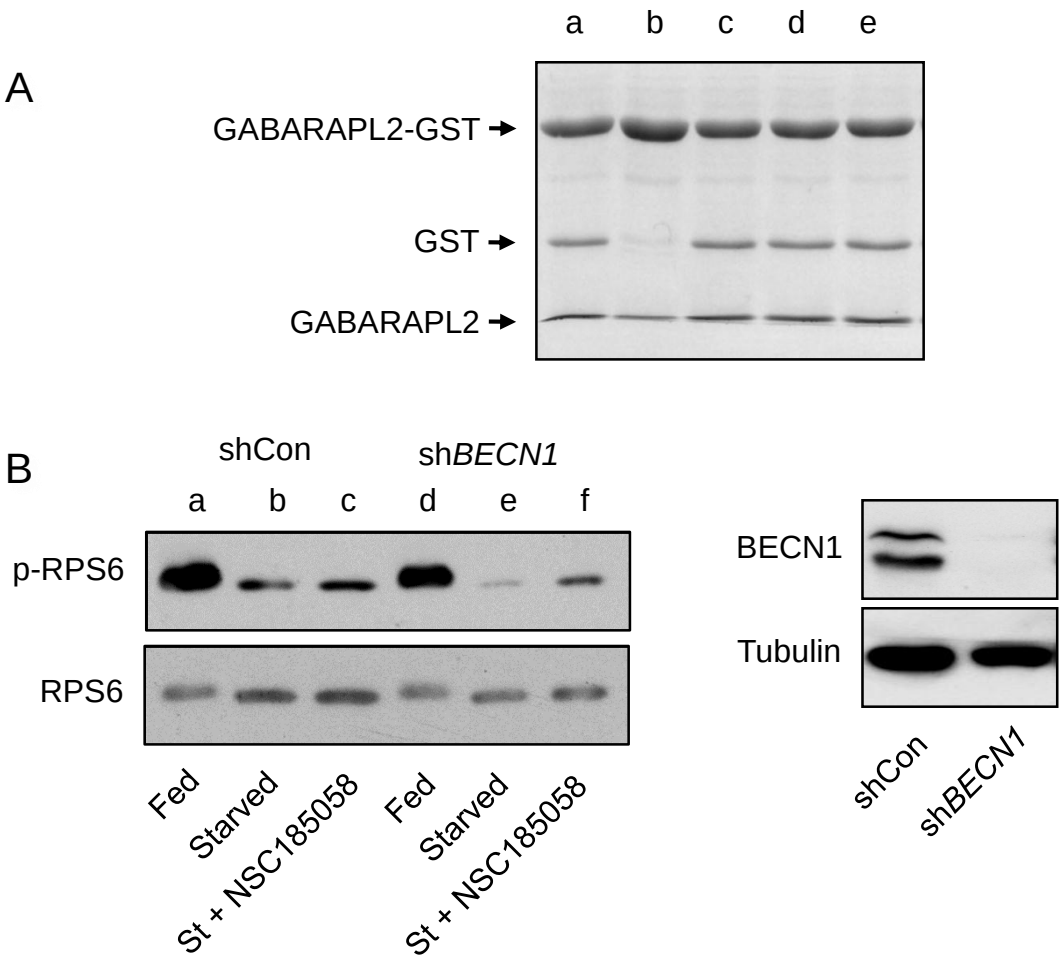
A
a b c d e
GABARAPL2-GST
GST
GABARAPL2
B
shCon
shBECN1
a b c d e f
p-RPS6
RPS6
Fed
Starved
St + NSC185058
Fed
Starved
St + NSC185058
BECN1
Tubulin
shCon
shBECN1
C
Saos-2
shCon-Saos
shATG4B-Saos-2
Percentage of Cells with Punctate FYVE-RFP Pattern
0
20
40
60
80
Fed
Starved
St + NSC185058
St + NSC377071
Starved
Starved

Figure S5. Specificity of ATG4B-targeted compounds. (**A**) The cleavage of GABARAPL2 - GST by purified ATG4A was assayed in the absence (lane a) and presence of NSC185058 (lane b), NSC377071 (lane c), NSC52086 (lane d), or NSC310196 (lane e) as described by Yin and coworkers.[5] The results suggest that NSC185058 suppresses ATG4A-mediated cleavage of GABARAPL2. (**B**) Knockdown of *BECN1* expression was evaluated by western blotting. shCon-Saos-2 and sh*BECN1*-Saos-2 cells were incubated under conditions of fed, starved, and starved plus NSC185058. After 4 h, the cells were solubilized, proteins separated by SDS-PAGE and the levels of ribosomal RPS6 and phosphorylated RPS6 (P-RPS6) evaluated on western blots. As predicted, starvation resulted in an inactivation of MTOR as determined by the dephosphorylation of RPS6 (lanes a and b). The results demonstrate that BECN1 had little effect on RPS6 phosphorylation under fed conditions (lanes a and d) and RPS6 dephosphorylation under starved conditions (lanes b and e). Furthermore, the results show that NSC185058 had no effect on starvation-induced RPS6 dephosphorylation (lanes b and c). (**C**) Saos-2, shCon-Saos-2, and sh*ATG4B*-Saos-2 cells transiently expressing FYVE-RFP were incubated under fed, starved, and starved conditions in the presence of NSC185058 or NSC377071. After 4 h, the cells were fixed and the FYVE-RFP labeled vacuoles visualized by fluorescence microscopy. The percentage of cells (50 to 100 cells counted per trial) with 3 or more FYVE-RFP dots are presented as the mean ± SEM (n = 3).

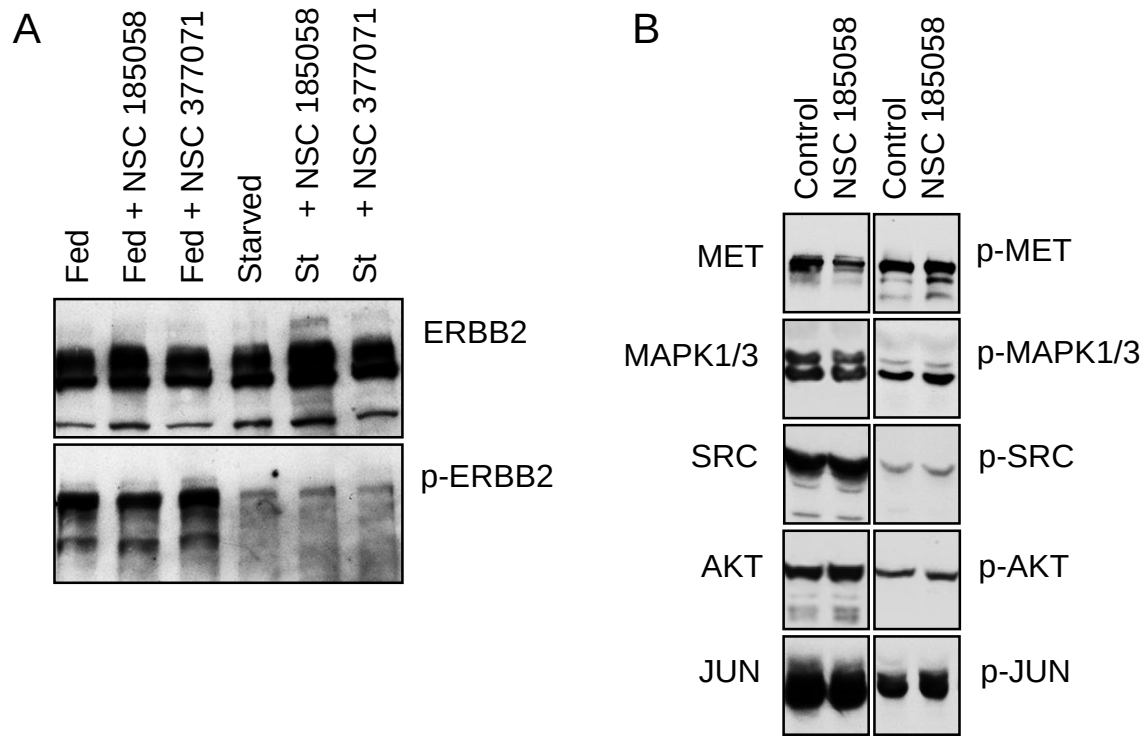

Figure S6. Activities of oncogenic kinases were unaltered in cells treated with NSC185058. (**A**) Saos-2 cells were incubated in nutrient-rich medium (Fed) or medium lacking amino acids and serum (Starved) in the absence and presence of NSC185058. After 4 h, the cells were solubilized and the levels of total and phosphorylated ERBB2 evaluated on western blots. The results demonstrate that NSC185058 had no effect on ERBB2 phosphorylation under fed conditions or ERBB2 dephosphorylation under starved conditions. The data show that NSC185058 is not acting through ERBB2 to inhibit starvation-induced autophagy. (**B**) Saos-2 cells were incubated in nutrient-rich medium in the absence and presence of NSC185058. After 4 h, the cells were solubilized and the levels of total and phosphorylated MET, MAPK1/3, SRC, AKT, and JUN evaluated on western blots. The results show that NSC185058 had no effect on the phosphorylated states of these kinases suggesting that this compound does not interfere with these cell proliferation and survival pathways.

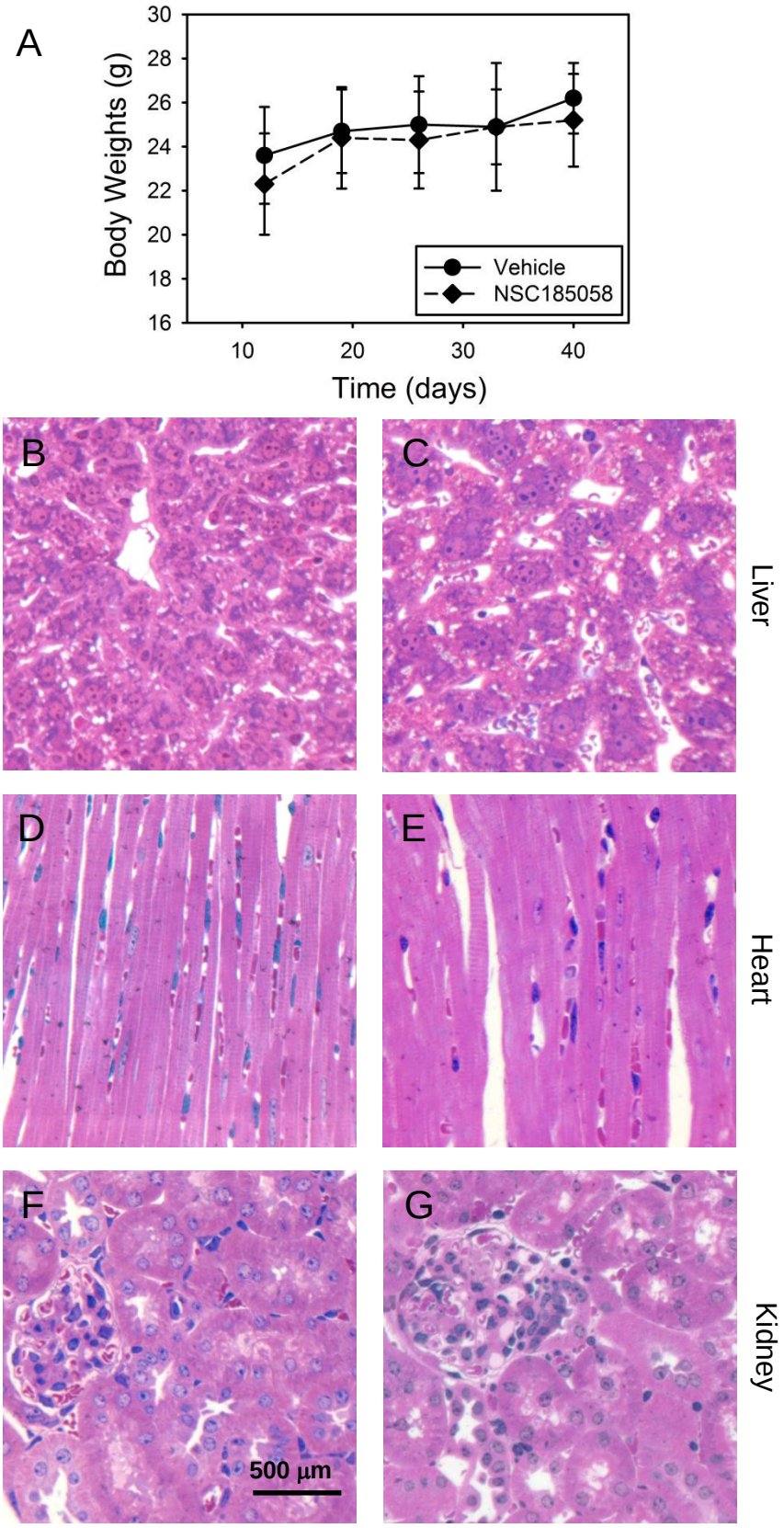
A
Body Weights (g)
30
28
26
24
22
20
18
16
10
20
30
40
Time (days)
Vehicle
NSC185058
B
C
D
E
F
G
Liver
Heart
Kidney
500 µm
Vehicle
NSC185058

Figure S7. NSC185058 treatment had no detrimental effects on mouse body weight and organ morphology. The toxicity of NSC185058 was assessed by monitoring body weight and observing morphology changes of the liver, heart, and kidney. (**A**) Body weights were monitored over 40 days (28 days of treatment). (**B to G**) Mice were euthanized after 34 days of treatment and biopsies of liver (**B and C**), heart (**D and E**), and kidney (**F and G**) were obtained from vehicle (**B, D, and F**) and NSC185058 (**C, E, and G**) treated mice. The samples were then fixed, embedded, sectioned and stained with H&E. Bar = 500 μm.

Table S1. ATG4B docked compounds.

Compound (NSC #)	Score	Comments
717529	-28.03	na
712422	-27.70	na
610509	-26.11	ne
24666	-25.70	Fig. S3
139109	-25.59	ne
522950	-25.13	na
377071	-25.02	Fig. S3
52086	-24.79	Fig. S3
72670	-24.23	na
141692	-23.78	ne
128761	-23.73	Fig. S3
402859	-23.68	na
185058	-23.38	Fig. S3
211925	-23.20	na
669590	-23.06	ne
280711	-22.93	na
67061	-22.91	ne
41434	-22.84	na
367416	-22.64	ne
310196	-22.51	Fig. S3

na, not available
ne, no effect

References

1. Susan PP, Dunn WA, Jr. Starvation-induced lysosomal degradation of aldolase B requires glutamine 111 in a signal sequence for chaperone-mediated transport. J Cell Physiol 2001; 187:48-58.
2. Aplin A, Jasionowski T, Tuttle DL, Lenk SE, Dunn WA, Jr. Cytoskeletal elements are required for the formation and maturation of autophagic vacuoles. J Cell Physiol 1992; 152:458-66.
3. Dunn WA, Jr. Studies on the mechanisms of autophagy: maturation of the autophagic vacuole. J Cell Biol 1990; 110:1935-45.
4. Dunn WA, Jr. Studies on the mechanisms of autophagy: formation of the autophagic vacuole. J Cell Biol 1990; 110:1923-33.
5. Li M, Hou Y, Wang J, Chen X, Shao ZM, Yin XM. Kinetics comparisons of mammalian Atg4 homologues indicate selective preferences toward diverse Atg8 substrates. The J Biol Chem 2011; 286:7327-38.